

*Invited talk to appear in "The Impact of Large-Scale Near-IR Sky Surveys", meeting held in Tenerife, Spain, April 1996, ed. F. Garzón*

## PRELIMINARY GALAXY EXTRACTION FROM DENIS IMAGES

G. A. MAMON, V. BANCHET, M. TRICOTTET AND D. KATZ  
*Institut d'Astrophysique  
98 bis Bd Arago, F-75014 Paris, France*

**Abstract.** The extragalactic applications of NIR surveys are summarized with a focus on the ability to map the interstellar extinction of our Galaxy. Very preliminary extraction of galaxies on a set of 180 consecutive images is presented, and the results illustrate some of the pitfalls in attempting an homogeneous extraction of galaxies from these wide-angle and shallow surveys.

### 1. Introduction

Near Infrared (NIR) surveys such as DENIS and 2MASS are extremely useful for extragalactic astronomy and cosmology, for mainly two reasons.

1. The extinction in the NIR bands is 11% ( $K_s$ ) to 28% ( $J$ ) of the visual extinction. This allows one with a wider view of the Universe, then allowed by optical surveys, limited to high galactic latitudes because of the extinction from interstellar dust of our Galaxy. This also allows a better view of external galaxies, as the light is unhampered by extinction from their own interstellar dust.
2. While optical light (in particular blue and ultraviolet) is extremely sensitive to massive very young (million year old) stars, NIR light is much less sensitive to recent star formation.

A caveat is in order for this second point: NIR light turns out to be more sensitive to 10 million year old bursts of star formation than other wavebands, because the very massive young stars evolve in that timescale onto the giant branch. This is well illustrated in synthetic spectra of iso-eval stellar populations (e.g. Bruzual & Charlot, 1993, Fig. 4a), in which the dispersion in waveband averaged intensity (*i.e.*, broad-band flux) for different ages of the stellar population is smallest in the NIR, with the exception

of the epoch at 10 million years. See also Knapen (in these proceedings) for an illustration of NIR luminous regions with recent star formation in the nuclei of external galaxies.

One could go to the mid-IR to avoid extinction by dust even further, but mid-IR light is sensitive to thermal emission from warm dust associated with recently formed stars and starting around the  $K$  band at 2.2 microns, ground-based observations are limited by thermal emission from the instrument.

## 2. Extragalactic applications

The applications of NIR surveys for extragalactic astronomy and cosmology have been described elsewhere (Mamon 1994, 1995, 1996; Schneider in these proceedings) and are briefly outlined again here.

The main extragalactic applications foreseen with DENIS are

- *A statistical sample of properties of NIR galaxies*  
The large sample size will help study correlations between properties.
- *The 2D structure of the local Universe.*  
Catalogs of groups and clusters will be obtained from the galaxy lists extracted from the survey images. Statistical measures of large-scale structure will be obtained (such as the angular correlation function and higher order functions, counts in cells, and topological measures). It will be interesting to see how all this 2D structure will vary with waveband, which will hopefully tell us about how structure is a function of waveband and indicate possible biases when going from one waveband to another. The alternative is that any such difference in 2D structure may be a reflection of selection effects, but we are working hard on avoiding this.
- *Color segregation*  
Instead of studying structure versus waveband, one can study the inverse problem of understanding colors as a function of structure, hence environment. Color segregation is a potentially powerful probe of three dimensional morphological segregation of galaxies in the Universe (*e.g.*, the cores of clusters being richer in ellipticals and poorer in spirals). Monte-Carlo tests are planned to find out whether one can recover such a morphological segregation from the 2D color segregation information that will be obtained from DENIS (despite the loss of information from projection effects, extinction, k-corrections, and tidally triggered star formation). If yes, then using  $I - J$  versus environment, with a sample of over  $10^5$  galaxies, DENIS would provide the largest sample for studying morphological segregation (typically limited to  $10^{3.5}$  galaxies today).

– *Normalization of galaxy counts at the bright-end*

Counting galaxies as a function of apparent magnitude provides better results at the faint-end than at the bright-end, simply because the bright-end suffers from very poor statistics (in the local uniform Universe, galaxy counts rise roughly as  $\text{dex}[0.6 m]$ ). If our Local Group sits in an underdense region, we should see a lack of galaxies at the very bright end of the galaxy counts, which is brighter than the DENIS complete/reliable extraction limit. The accepted standards for galaxy counts, arising from the APM (Maddox et al. 1990) and COSMOS (Heydon-Dumbleton et al. 1989) surveys have yielded bright-end counts that were inconsistent with the intermediate magnitude counts, for a uniform Universe with no abnormally strong galaxy evolution. In recent studies (Bertin & Dennefeld 1996; Gardner et al. 1996), the bright-end normalization in  $B$  is roughly twice as large as in the APM and COSMOS counts (the discrepancy is apparently due to poor correction for non-linear plate response in the first two studies), and in agreement with simply extrapolated fainter counts. However, the error bars still remain large, and very wide-angle surveys such as DENIS and 2MASS will bring them down. Moreover, two recent studies (Lidman & Peterson 1996; Gardner et al. 1996) display strong discrepancy of the bright-end counts in  $I$  (see. Figure 1).

– *Mapping interstellar extinction*

Among the many ways one can map the interstellar extinction in our Galaxy, one is to use galaxy counts (Burstein & Heiles 1978, 1982), since the count normalization is shifted downwards when galaxies are extinguished. Galaxy counts are tricky extinction calibrators, because of intrinsic variations of galaxy counts (the correlation of the galaxy distribution implies fluctuations of counts in cells that are greater than Poisson). Also, the low sensitivity of NIR surveys implies the need of very large solid angles for significant counts, hence any extinction map would be of very poor angular resolution. On the other hand, galaxy colors may provide the best way to map the interstellar extinction, as they redden with extinction (this method is hampered by any intrinsic color segregation). The maximum extinction that can be probed using  $I - J$  colors is

$$A_V^{\max} = \frac{I_{\text{lim}} - J_{\text{lim}} - (I - J)_0}{E(I - J)/A_V} \simeq 9 ,$$

with  $I_{\text{lim}} \simeq 17.0$ ,  $J_{\text{lim}} \simeq 14.5$ ,  $(I - J)_0 \simeq 0.7$ , and  $E(I - J)/A_V = 0.2$ . Beyond this extinction, we start missing galaxies in the more extinguished  $I$  band. The uncertainty on the extinction comes from the uncertainty on the mean galaxy color, which in turn arises from

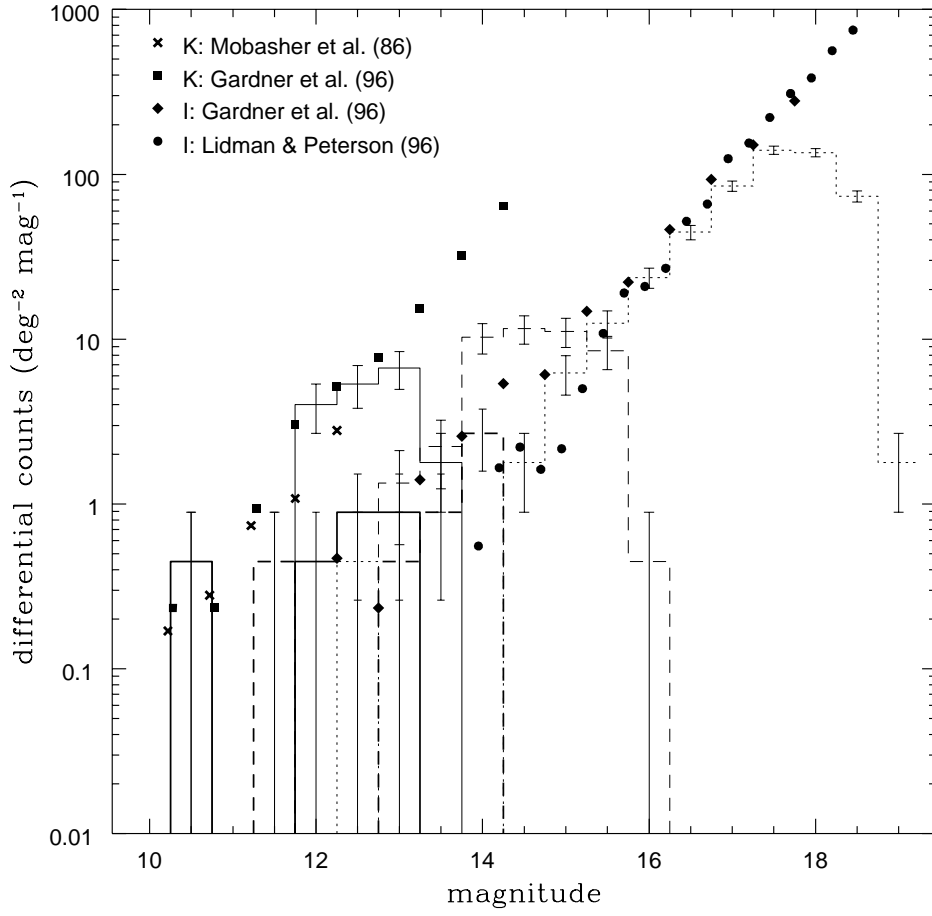


Figure 1. Counts of candidate galaxies for strip 3081 of 180 consecutive images. *Solid*, *dashed*, and *dotted thin* histograms show our DENIS counts in *K*, *J*, and *I*. The *thick* histograms refer to objects also seen in the bluer band(s) (*I* and *J* for *K* and *I* for *J*). For comparison are also shown *K* counts by Mobasher et al. (1986) and Gardner et al. (1996), and *I* counts by Lidman & Peterson (1996) and Gardner et al. (1996). All surveys have similar areas, so the error bars have roughly the same sizes for given ordinate.

the width of the color distribution and the photometric errors. With  $\Delta I \simeq \Delta J \simeq 0.2$ , and a similar dispersion in intrinsic colors, a sample of  $N$  galaxies will yield an uncertainty

$$\Delta A_V = N^{-1/2} \frac{\Delta(I - J)}{E(I - J)/A_V} \simeq 2 N^{-1/2}. \quad (1)$$

Given the expected unextinguished counts in the *J* band,  $N(< J) \simeq$

$5 \times \text{dex}[0.6(J - 14.5)] \text{ deg}^{-2}$ , using  $A_J = 0.28 A_V$ , the extinguished counts fall by a factor  $\text{dex}(0.6 \times 0.28 A_V)$ , while the galaxy extraction limit will fall by roughly  $0.28 A_V$  magnitude, hence the counts of extracted galaxies in extinguished regions will vary roughly as

$$N \simeq 5 \text{ dex}(1.2 \times 0.28 A_V) (\Delta\theta)^2, \quad (2)$$

where  $(\Delta\theta)^2$  is the solid angle in  $\text{deg}^2$ . For an accuracy  $\Delta A_V$ , one requires (eqs. [1] and [2]) an angular resolution

$$\Delta\theta \simeq \frac{0.9}{\Delta A_V} \text{dex}[-(0.6 \times 0.28 A_V)] \text{ deg} . \quad (3)$$

The results are shown in Table 1.

TABLE 1. Angular resolution required for mapping extinction (eq. [3])

$A_V$	1	2	5	5	5	9	9	9
$\Delta A_V$	0.2	0.2	0.1	0.2	0.5	0.1	0.2	0.5
$\Delta\theta$ (deg)	3.03	2.06	1.29	0.65	0.26	0.28	0.14	0.06

### 3. Galaxy pipelines

#### 3.1. GOAL

The DENIS galaxy pipeline is still under development. It is a 2-pass pipeline described below:

In the first pass, all sources extracted in the LDAC pipeline are checked for a minimum area above threshold, required for reliable galaxy detection (the values are obtained by image simulations). Kron photometry is applied on these sources with parameters optimized from image simulations. Star galaxy separation is performed in two manners: 1) by classical methods, using a combination of maximum pixel-intensity (corrected for the position of the object centroid relative to the pixel center), area above threshold, and full-width half-maximum, given the magnitude. 2) by neural networks trained on simulated images (Bertin 1996). So far, neural networks prove superior, but also make mistakes for bright or intermediate flux galaxies that the classical methods avoid.

In the second pass, stars are removed from the images, by masking the saturated stars and subtracting the PSF from non-saturated ones. Then large-scale smoothing is applied to the images, which allows one to recover

face-on late-type spiral galaxies, that are otherwise invisible in  $K$ . Object detection is done with parameters optimized to avoid fragmentation of the brighter objects (due to photon noise). Kron photometry is performed again. Obviously no star galaxy separation is required for this second list, although checks will be made.

### 3.2. PRELIMINARY PIPELINE

We now present preliminary results from the extraction with a preliminary pipeline, which is as follows:

We first filter the images to remove cosmics and bad pixels. We then use the easy-to-use *SExtractor* package (Bertin & Arnouts 1996). Again we set a minimum area above threshold for galaxies and smooth the images with a conical  $3 \times 3$  filter in the  $I$  band, and the convolution of that filter with a  $3 \times 3$  boxcar in the  $J$  and  $K$  bands (because a  $3 \times 3$  boxcar is required to transform the interlaced images of 9 sub-images in these 2 bands into images obtained by co-adding the sub-images). The threshold is set at  $3\sigma$  on the smoothed images (as optimized from simulated images), and Kron photometry is applied with parameters optimized from the simulated images. *SExtractor* uses neural networks for the star galaxy separation, and assumes a constant point-spread-function (PSF) within and among strips of 180 consecutive images. The results below are for objects with *SExtractor* stellarity index  $< 0.1$ .

## 4. Results on two strips

Figure 2 shows the superposition of the positions of candidate galaxies over 180 consecutive images of a good quality high galactic latitude strip (3081). Careful inspection of Figure 2 indicates that there is vignetting in  $I$  and an excess of objects on the right-side of the frames in  $K$ , which is due to a small linear variation of the PSF along Right Ascension in this strip.

Six candidate galaxies are seen in all three wavebands. Five out of six are in the same upper-right quadrant of their respective images, which is probably a signature of PSF variations. The six candidates are shown in Figure 3. The  $K$  images clearly limit the galaxies to their central regions. The fourth candidate galaxy from the top appears to be a double star (see the  $I$  image on the left).

The colors of the six galaxy candidates are shown in Figure 4. While at least two of the galaxies in Figure 3 are clearly edge-on spirals, their colors are slightly redder than ellipticals. Because the low sensitivity in  $K$  limits the visibility and photometry of galaxies to their central regions, one would have expected that the  $J - K$  colors be too blue, which is not seen.

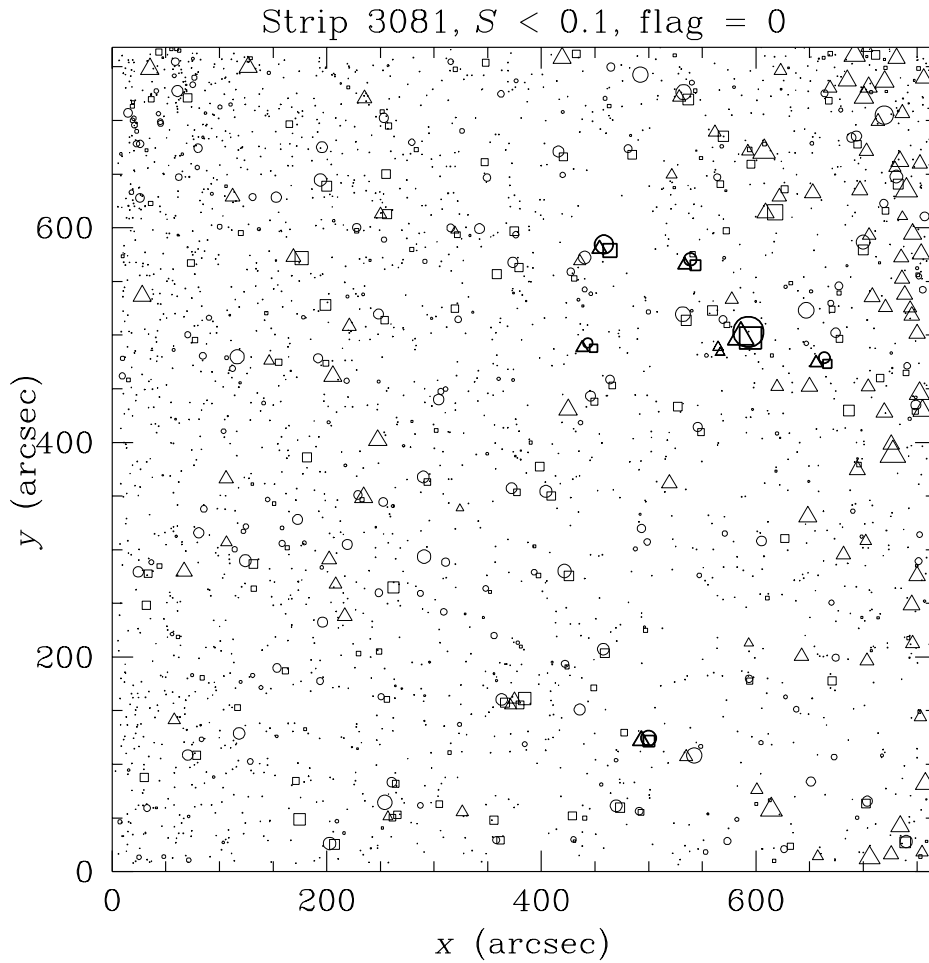


*Figure 2.* Positions of galaxy candidates in 180 superposed images. Objects extracted in  $I$ ,  $J$ , and  $K$  are shown as *circles*, *squares*, and *triangles*, respectively. The sizes of the symbols are scaled to their magnitude, with the same normalization for the brightest object of each waveband. Objects that appear galaxy-like in all three wavebands are shown with *thick symbols*.

In Figure 1 are shown galaxy counts for this strip (we omit here objects at less than  $100''$  from the image edges, yielding a solid angle of  $4.5 \text{ deg}^2$  for the strip). The ‘raw’  $K$  counts agree better with previous work than the ‘constrained’  $K$  counts. These raw counts are however likely to be severely contaminated by stars. The constrained object list is thus highly incomplete. The  $I$  band counts show a good agreement with those of Lidman & Peterson (1996) and Gardner et al. (1996), suggesting a completeness limit

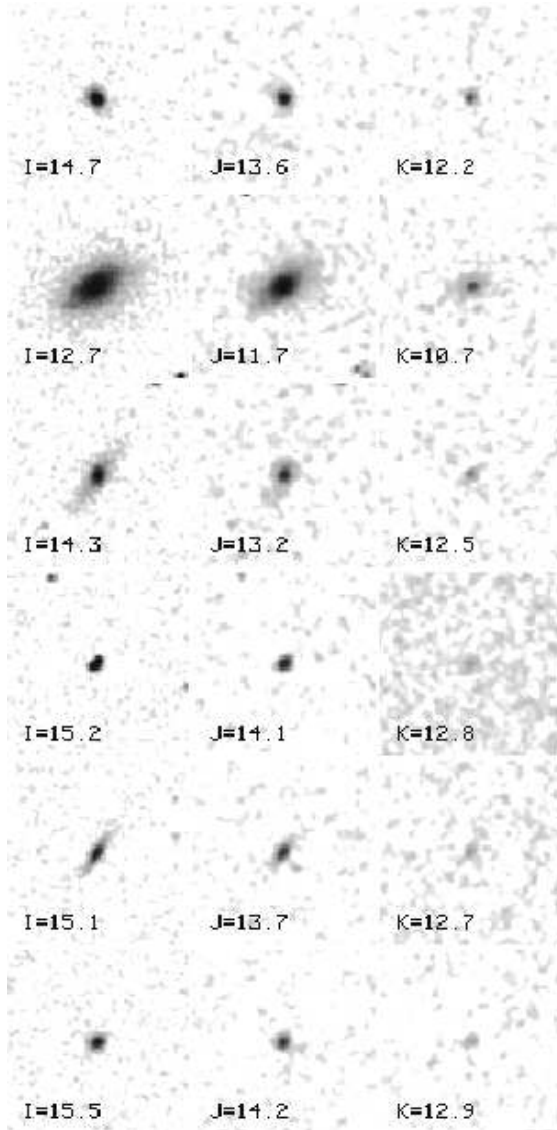


*Figure 3.* Six candidate galaxies from strip 3081 of 180 consecutive images in  $I$  (left),  $J$  (middle), and  $K$  (right). Kron photometry is given for each object. Greyscale is logarithmic from 1.5 to  $50\sigma$ . Images are smoothed with the filters discussed in section 3.2.

of  $I \simeq 16.75$ .

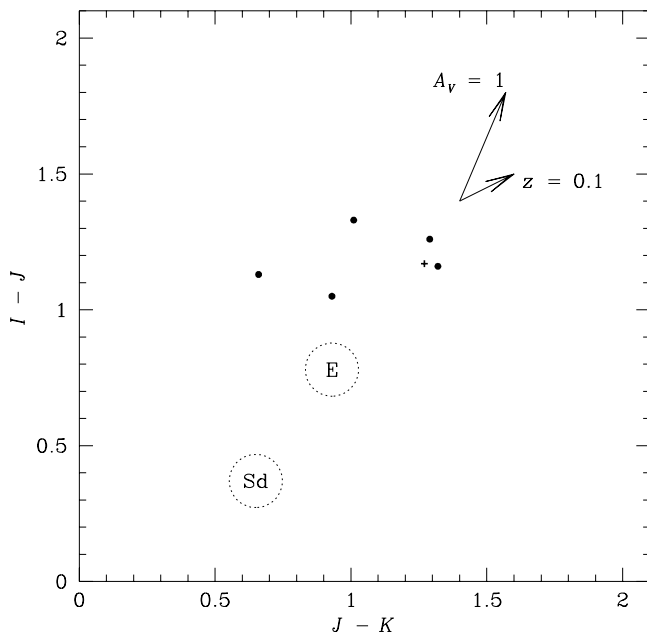


*Figure 4.* Color-color diagram of strip 3081. The *cross* is for the candidate galaxy appearing as a double star. The typical colors (from the compilation of Yoshii & Takahara 1988, see also Peletier in these proceedings) of ellipticals (E) and late-type spirals (Sd) are shown. Arrows indicate one visual-magnitude of extinction ( $A_V = 1$ ) and the effects of differential  $k$ -correction ( $z = 0.1$ ).

## 5. Discussion and conclusions

The incompleteness of our extraction in  $K$  illustrates the inadequacy of our preliminary extraction pipeline. We processed a second strip, of poor quality (with strong PSF variations across the images) and obtained ‘constrained’ counts in  $K$  that matched better previous determinations, and suggested a completeness limit of  $K \simeq 12.25$ . We have recently begun to incorporate modeling of the PSF (see Borsenberger, in these proceedings) over a number of subsequent images into our star/galaxy separators. Since over 99% of objects are stars, we perform an iterative asymmetric rejection of large PSFs before modeling it. Preliminary tests yield rms residuals less than  $0.15''$ , after optimizing for the minimum area of objects to consider and the number of subsequent images on which the modeling is done. We expect the new star/galaxy separators to have much more uniform galaxy distributions over the images in comparison with what is shown in Figure 2.

We thank Emmanuel Bertin for numerous useful discussions.

## References

- Bertin, E. 1996, *PhD thesis, University of Paris 7*  
Bertin, E. & Arnouts, S. 1996, *A&AS*, **117**, 393  
Bertin, E. & Dennefeld, M. 1996, *A&A*, in press (astro-ph/9602110)  
Bruzual A., .G. & Charlot S. 1993, *ApJ*, **405**, 538  
Burstein, D. & Heiles, C. 1978, *Astrophys. Lett.*, **19**, 69  
Burstein, D. & Heiles, C. 1982, *AJ*, **87**, 1165  
Gardner, J.P., Sharples, R.M., Carrasco, B.E. & Frenk, C.S. 1996, *MNRAS*, in press (astro-ph/9606067)  
Heydon-Dumbleton, N.H., Collins, C.A. & MacGillivray, H.T. 1989, *MNRAS*, **238**, 379  
Lidman, C.E. & Peterson, B.A. 1996, *MNRAS*, **279**, 1357  
Maddox, S.J., Sutherland, W.J., Efstathiou, G., Loveday, J & Peterson, B.A. 1990, *MNRAS*, **247**, 1p  
Mamon, G.A., 1994, *ApSS*, **217**, 237  
Mamon, G.A., 1995, in *Wide-Field Spectroscopy and the Distant Universe*, ed. S.J. Maddox & A. Aragón-Salamanca (Singapore: World Scientific), p. 73.  
Mamon, G.A., 1996, in *Spiral Galaxies in the Near-IR* ed. D. Minniti & H.-W. Rix (Garching: ESO), p. 195.  
Mobasher, B., Sharples, R.M. & Ellis, R.S. 1986, *MNRAS*, **223**, 11  
Yoshii, Y & Takahara, F. 1988, *ApJ*, **326**, 1